buildings

Article

Study on the Influence of High-Altitude Helical Tunnel Curvature on Jet Fan Spatial Layout

Zijian Wang [1], Qi Liu [1], Hao Li [1,*], Bin Zhang [1], Liming Wu [2], Sichang Wang [1] and Chaolin Jia [3]

[1] School of Civil Engineering and Architecture, Chongqing University of Science & Technology, Chongqing 401331, China; 2013016@cqust.edu.cn (Z.W.); 2021206053@cqust.edu.cn (Q.L.); 2020007@cqust.edu.cn (B.Z.); 2011015@cqust.edu.cn (S.W.)
[2] School of Urban Construction Engineering, Chongqing Technology and Business Institute, Chongqing 400052, China; wulm@cqtbi.edu.cn
[3] Chongqing Chuanjiu Construction Co., Ltd., Chongqing 401120, China; 13983706022@163.com
* Correspondence: 2022206036@cqust.edu.cn

Abstract: During the operational ventilation process of high-altitude helical tunnels, the installation method of jet fans is a key factor in determining the ventilation efficiency of the tunnel. In this study, the CFD numerical simulation method is adopted to establish three-dimensional ventilation models of helical tunnels with different curvature radii. Through orthogonal experiments, the effects of tunnel curvature radius on the characteristics of the air jet flow field, under the coupled influences of factors such as lateral spacing of jet fans, vertical height of fans, longitudinal spacing, and lateral offset, are investigated. The results show that when R = 500 m, 600 m, 700 m, and 800 m, the longitudinal spacing has the most significant impact on ventilation efficiency, followed by vertical height, with lateral offset and fan spacing having the least impact. The optimal spacing and vertical height of the fan groups remain consistent under different curvature radii, at 1.25D (fan diameter) and 15 cm, respectively. The optimal longitudinal spacing of the fan groups is 90 m, 90 m, 135 m, and 90 m, respectively. Shifting the fan groups 0.25 to 0.75 m towards the inner side of the tunnel helix (for R < 700 m) can optimize the flow field distribution within the tunnel. Finally, expressions for the relationship between the helical radius and the lateral offset and longitudinal spacing of the fan groups are established for the optimal installation parameters of fan spatial positions under different helical tunnel radii.

Keywords: helical tunnel; ventilation efficiency; orthogonal experiment; ventilation optimization; numerical simulation

check for updates

Citation: Wang, Z.; Liu, Q.; Li, H.; Zhang, B.; Wu, L.; Wang, S.; Jia, C. Study on the Influence of High-Altitude Helical Tunnel Curvature on Jet Fan Spatial Layout. *Buildings* **2024**, *14*, 2160. https://doi.org/10.3390/buildings14072160

Academic Editor: Bingxiang Yuan

Received: 23 May 2024
Revised: 8 July 2024
Accepted: 11 July 2024
Published: 13 July 2024

1. Introduction

The swift advancement of China's highway tunnel industry has seen the extensive utilization of longitudinal ventilation techniques, in which jet fans are instrumental. In high-altitude regions, characterized by intricate terrain and severe climatic conditions, conventional tunnel designs may encounter numerous challenges. To reduce the incidence of geological hazards such as landslides and debris flows, and to manage elevation changes effectively, enabling tunnels to climb at secure gradients, a spiral design has been implemented in some tunnels to tackle the problem of excessive tunnel gradients. The engineering of these uniquely structured tunnels is vital for ensuring transportation safety in the harsh climatic conditions prevalent at high altitudes. Within helical tunnels, jet fans can effectively generate strong airflow, maintaining the efficient operation of ventilation systems and ensuring fresh and clean air within the tunnel through smoke extraction functions. However, differences in fan parameter configuration and layout can alter the development characteristics of airflow and parameters such as the fan pressure coefficient, ultimately affecting the fan's pressure boosting efficiency, as indicated by Xu et al. (2021) [1]. Therefore, in the ventilation of helical tunnels, the question of how to optimize the layout of jet fans to achieve the best ventilation effect has received widespread attention from scholars.

Several researchers have conducted studies on the layout of fans within helical tunnels. To enhance the pressure boosting performance of jet fans, Davies et al. (1963) [2] first discovered and studied the phenomenon of vortex alternation in jet flows, providing a theoretical basis for the study of jet flow expansion. Mutama et al. (1996) [3] conducted experimental studies on the aerodynamic characteristics of jet fans in a wind tunnel, showing that the distance between the fan and the tunnel wall has a significant impact on the induced airflow characteristics of jet fans. Wang et al. (2010) [4] numerically simulated the aerodynamic characteristics of an airflow induced by jet fans in curved tunnels, showing that due to the interaction between the airflow and the curved tunnel walls, the pressure downstream of the jet fan exhibits a non-monotonic trend, and the velocity downstream of the jet fan exhibits an asymmetric distribution. To optimize the pressure boosting effect of jet fans, Wang et al. (2012) [5] further studied the optimal deflection angle of fans in curved tunnels, finding that a deflection of 3° yielded the best pressure boosting effect. Li et al. (2019) [6] used the FLUENT2019R3 software to study the development characteristics of airflow in urban small-radius highway tunnels. The results showed that there are varying degrees of negative pressure and low-speed areas in curved tunnels, which can lead to backflow, and with increasing radius, the flow field in curved tunnels gradually becomes more uniform. Ding et al. (2017) [7] used CFD numerical simulation to reveal that the pressure boosting characteristics of small-radius curved tunnels differ from those of straight tunnels, and the lateral spacing of fans can be adjusted according to the number of fans. Chen et al. (2021) [8] used CFD2021R1 software to study the effects of various parameters on the flow field and pressure boosting, and provided fan layout recommendations for curved tunnels with radii of 65 m and 85 m. Xu et al. (2023) [9] established a full-size tunnel model using FLUENT, showing that the airflow in curved tunnels is asymmetric, and shorter distances are required to achieve uniform airflow in small-radius tunnels, with a more significant increase in pressure coefficient. Chen et al. (2021) [10] found that appropriate inclination angles can enhance the pressure boosting effect and reduce wall shear stress. Gao et al. (2021) [11] found that the most significant factors affecting the pressure reduction coefficient are the jet angle and vertical height. Li et al. (2023) [12], combined with orthogonal experiments, studied the effects of factors such as the lateral spacing, offset distance, and deflection angle of jet fans on fan efficiency in different small-radius curved tunnels. The results showed that the degree of influence of each factor on fan ventilation efficiency varies with different curvature radii, with poorer ventilation efficiency observed in tunnels with smaller curvature radii. In the realm of ventilation, the deployment of effective monitoring and optimization techniques is paramount for safeguarding the internal environment within tunnels. Our research leverages sophisticated computational approaches to scrutinize the ventilation features of spiral tunnels, resonating with contemporary research trajectories, particularly the state-of-the-art technologies in European tunnel ventilation monitoring, as highlighted by Rosso et al. (2022) [13] and Habashneh et al. (2024) [14]. Within their investigation, Rosso et al. (2022) [15] conducted an exhaustive review of tunnel ventilation monitoring, underscoring the capacity of deep learning technologies to augment the precision of monitoring endeavors. In addition, Habashneh et al. (2024) [14] introduced innovative vistas for the design of steel beams subjected to elevated temperatures via cutting-edge elasto-plastic topology optimization methodologies. Collectively, these contributions substantiate the proposition that the integration of intelligent algorithms and optimization strategies can markedly augment the efficacy of tunnel ventilation systems.

In summary, the arrangement of jet fans significantly affects the ventilation efficiency and airflow characteristics of helical tunnels, primarily including factors such as lateral spacing, longitudinal spacing, lateral offset distance, the vertical height of the fans, and the deflection angle of the fans relative to the tunnel curve. These factors influence the performance and effectiveness of the ventilation system, thereby impacting the airflow and air quality within the tunnel. However, the current academic focus lies in the optimization of jet fans specifically tailored to the cross-sectional layout of tunnels with specific curvatures, with less emphasis on the optimization of the spatial layout for jet fans in tunnels with varying curvatures. Therefore, it is necessary to conduct in-depth research on the optimization of the spatial layout for jet fans in helical tunnels under the coupling effects of multiple factors. This will provide a comprehensive understanding of the optimal layout schemes under different curvature conditions, which can improve the efficiency and performance of ventilation systems, thereby reducing operational costs. The research findings can serve as a reference for the construction of similar high-altitude helical tunnels.

The ventilation effectiveness of jet fans is closely related to their spatial layout within helical tunnels. Jet ventilation in helical tunnels differs from turbulent free jets, as it involves the aerodynamics of jets in confined spaces. While these jets share some basic characteristics with free jets, their behavior is inherently different due to boundary condition constraints, resulting in more complex dynamic behaviors within helical tunnels (Wang, 2010) [16].

In response to the unique conditions of helical tunnels, research has been conducted to systematically analyze unit ventilation segments (Wang, 2000) [17]. This ventilation unit mainly consists of a jet-induced ventilation section and a pressure ventilation section, as illustrated in Figure 1. During the jet-induced phase, the airflow exhibits characteristics of entrainment and diffusion, resulting in significant induction effects that play a core role in ventilation performance. This characteristic is similar to free jet flows. In the pressure ventilation phase, the pressure boosting features induced by jet flow pressure changes are demonstrated. In the layout of curved tunnels, the non-uniformity of flow is particularly critical in both ventilation phases, with its complexity being more pronounced than in straight tunnels.

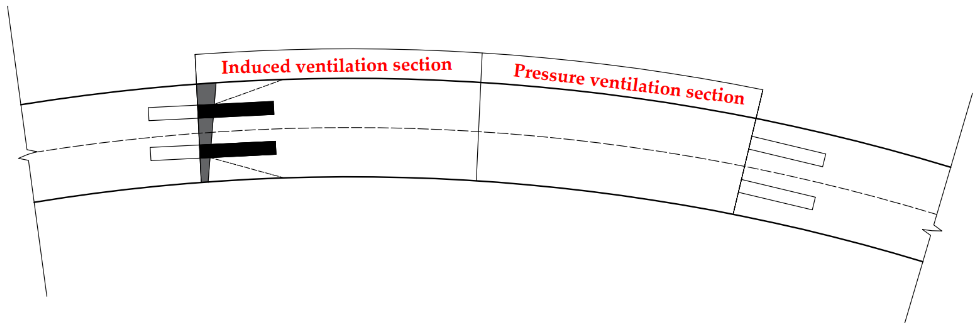

Figure 1. The flow structure of the ventilation section in a spiral tunnel element (Wang, 2010) [16].

2. Establishment of CFD Model for High-Altitude Helical Tunnels

2.1. Establishment of Physical Model

Based on the structural parameters of a helical tunnel project in the northwest region of China, a computational model with a scale of 1:1 is constructed using the computational fluid dynamics (CFD) software FLUENT. In this model, the computational length is set to 500 m, and the helical curvature radius R is varied at 500 m, 600 m, 700 m, and 800 m. The geometric model of the tunnel is shown in Figure 2. Two groups of jet fans (each consisting of two fans) are arranged inside the tunnel. The first group of fans is fixed at a position 50 m from the tunnel entrance, while the specific positions of the two groups of fans are designed according to an orthogonal table. The computational model in this study employs unstructured mesh generation, with a mesh size of 0.4 m specified for the tunnel and 0.1 m for the jet fans. It should be clarified that while the mesh refinement accentuates the representation of these critical areas visually, it does not indicate the implementation of variable mesh sizing within the simulation. Designed to capture detailed flow characteristics within the tunnel, the mesh maintains uniformity across the simulation domain. A schematic representation of the mesh for the tunnel ventilation model is presented in Figure 3. The jet fans are simulated using cylindrical models with a diameter of 1.12 m and a length of 3 m.

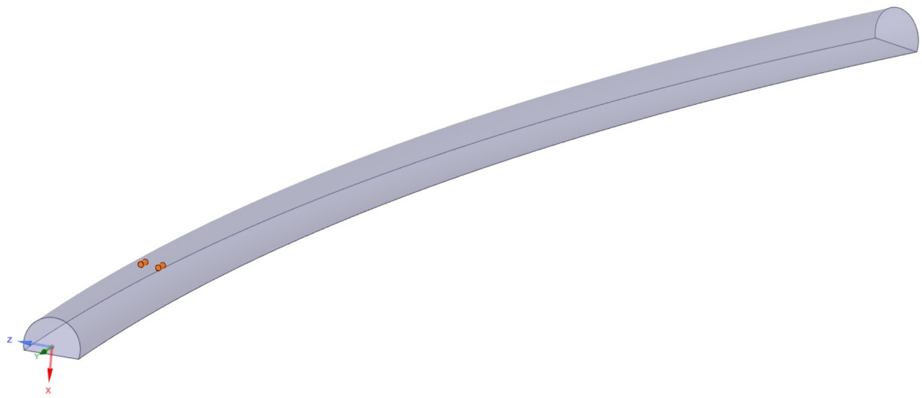

Figure 2. Geometric modeling of the tunnel.

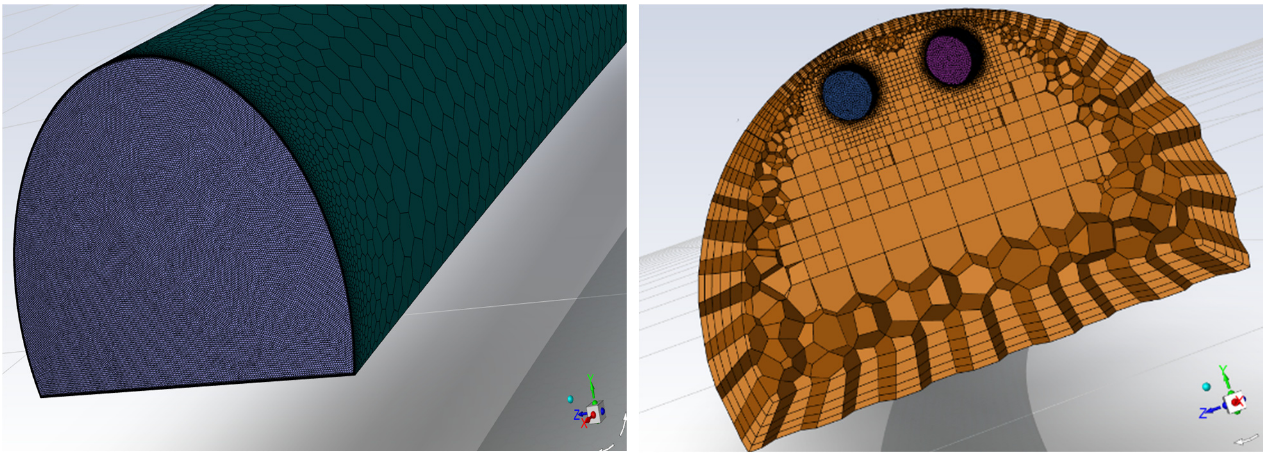

Figure 3. Schematic diagram of meshing at tunnel and fan.

2.2. Boundary Conditions

The grid generated is imported into the CFD software FLUENT for iterative calculations. The model utilizes a pressure-based solver with a two-equation turbulence model. The velocity–pressure coupling is performed using the Semi-Implicit Method for Pressure-Linked Equations (SIMPLE) algorithm. The convergence criterion for the residual values is set based on the requirements. Typically, the residual values are set to be less than 1×10^{-6}.

In the CFD simulation, the fluid density is a critical parameter that directly affects the accuracy of the results. In high-altitude regions, where air pressure is lower, air density decreases accordingly. To ensure accuracy, proper corrections must be applied to the fluid density. The corrected air density after altitude adjustment can be calculated as per reference (Gao et al., 2021) [11].

The selected jet fan model is of Type 1120, with a fan speed set to a specified value. The fan blades are assumed to be smooth walls, while the tunnel walls are considered concrete walls with a roughness height of 0.002 m and a roughness constant of 0.5.

The determination of boundary conditions in our study was guided by an array of references, encompassing prior research, industry benchmarks, and empirical data. This comprehensive approach ensures that the boundary conditions are both realistic and specifically applicable to the requirements of our investigation (Gao et al., 2021) [11]. The boundary conditions are summarized in Table 1.

Table 1. Computational model boundary condition settings.

Model Position	Boundary Conditions	Parameters
Tunnel Entrance	Velocity Inlet Boundary	3 m/s
Tunnel Exit	Pressure Outlet Boundary	0
Fan Inlet	Velocity Inlet Boundary	−30 m/s
Fan Outlet	Velocity Inlet Boundary	30 m/s
Tunnel Bottom and Top	Wall Boundary	The average roughness height of the wall surface is 0.002 m The roughness constant of the wall surface is 0.5

2.3. Calculation Conditions

High-altitude helical tunnel ventilation simulations utilize an orthogonal experimental design. The application of an orthogonal experimental design effectively reduces the number of model tests while determining the optimal levels of various influencing factors and assessing their relative importance. In this study, four factors are chosen for analysis: lateral spacing of fan groups (L), vertical height (H), longitudinal spacing (S), and lateral offset (K). The lateral spacing of fan groups (net spacing) L is expressed as multiples of the fan diameter D for standardization and comparison purposes. The direction of the lateral offset of fan groups is consistently towards the inner spiral of the tunnel axis (Gao et al., 2021) [11]. The schematic diagrams of jet fan installation positions, fan offset distances, and longitudinal spacing are shown in Figures 4 and 5.

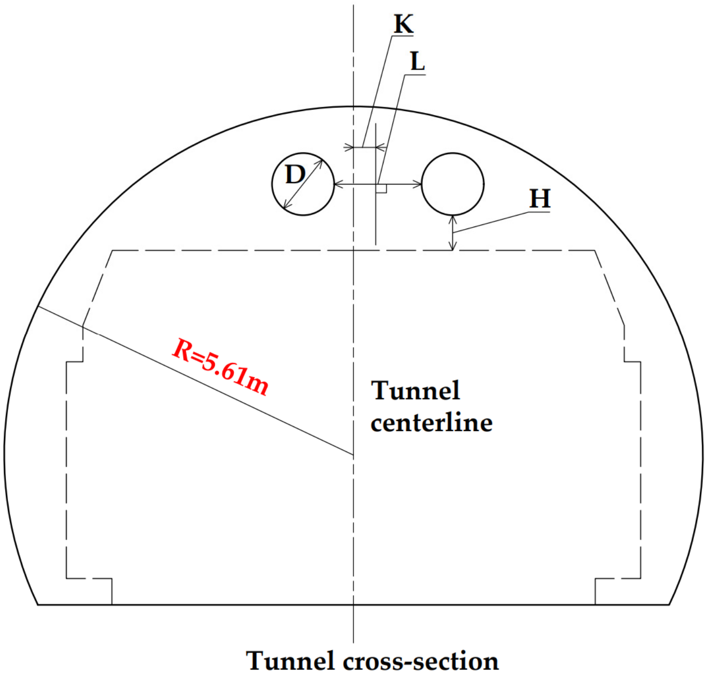

Figure 4. Tunnel cross-section.

In the “Design Guidelines for Highway Tunnel Ventilation” ($JTG/TD70/2-02-2014$) [18], the arrangement of jet fans in the tunnel space is specified as follows:

(1) H should be greater than or equal to 15 cm.
(2) L should not be less than 1 times the diameter of the fan impeller.
(3) For jet fans with D > 1000 mm, S should preferably be greater than 150 m.
(4) The longitudinal spacing (S) for jet fans with D < 1000 mm, or for jet fans located within the curved sections of a tunnel, should not exceed 100 m.

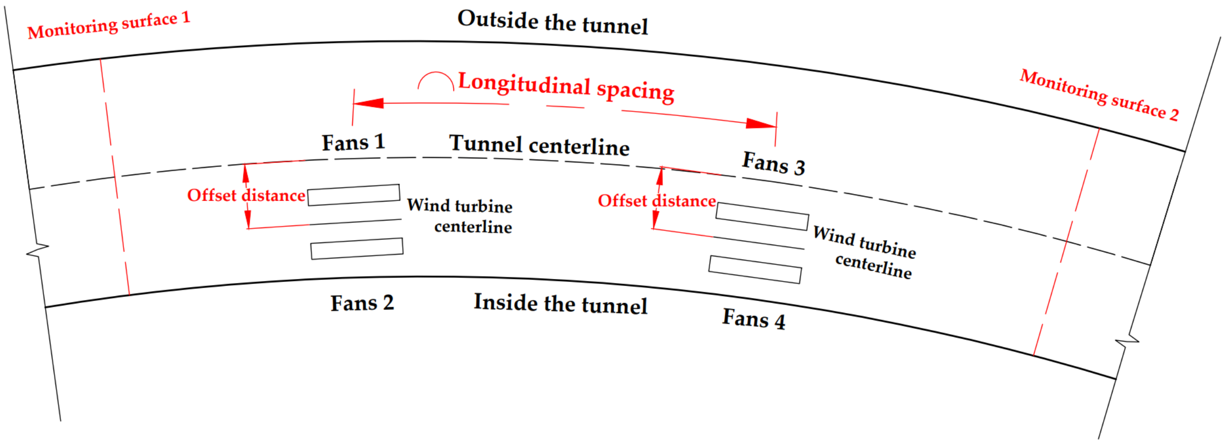

Figure 5. Schematic of jet fan offset distance.

When selecting the longitudinal spacing distance for jet fans, reference was made to the research by the scholars Li et al. (2023) [12], who used the boosting capability as the evaluation criterion. It was found that in curved tunnels, the optimal longitudinal spacing distance for fans is 130 m for better ventilation effectiveness. Therefore, the value of S in this study exceeds the specified value. Based on the aforementioned standards and considering multiple helical tunnels with different curvature radii, multiple sets of orthogonal experiments were conducted. The selected factors and their levels are detailed in Table 2.

Table 2. Factors and levels.

Levels	Factors			
	L	H	S	K
1	1.25D	15 cm	50 m	0 m
2	1.50D	25 cm	100 m	0.25 m
3	1.75D	35 cm	150 m	0.50 m
4	2.00D	45 cm	200 m	0.75 m

In order to ascertain the impact of the spiral radius on the spatial positioning parameters of the fans, the experiment utilized orthogonal testing with models of tunnels featuring varying spiral radii. An ‘empty column’ was designated for the purpose of variance analysis, and the numerals 1 through 4 within this column represent distinct experimental trials, thereby ensuring the systematic and reproducible aspect of the experimental design. According to the orthogonal experimental table, each tunnel with a different curvature radius was simulated 16 times, totaling 64 simulations. A 5-factor, 4-level orthogonal experimental table was selected, denoted as $L_{16}(4^5)$, as shown in Table 3.

Table 3. Orthogonal tables.

Column	1	2	3	4	5
Factors	**L**	**H**	**S**	**K**	**Empty Column**
Experiment 1	1.25D	15 cm	50 m	0 m	1
Experiment 2	1.25D	25 cm	100 m	0.25 m	2
Experiment 3	1.25D	35 cm	150 m	0.50 m	3
Experiment 4	1.25D	45 cm	200 m	0.75 m	4
Experiment 5	1.50D	15 cm	100 m	0.50 m	4
Experiment 6	1.50D	25 cm	50 m	0.75 m	3
Experiment 7	1.50D	35 cm	200 m	0 m	2
Experiment 8	1.50D	45 cm	150 m	0.25 m	1

Table 3. *Cont.*

Column	1	2	3	4	5
Factors	**L**	**H**	**S**	**K**	**Empty Column**
Experiment 9	1.75D	15 cm	150 m	0.75 m	2
Experiment 10	1.75D	25 cm	200 m	0.50 m	1
Experiment 11	1.75D	35 cm	50 m	0.25 m	4
Experiment 12	1.75D	45 cm	100 m	0 m	3
Experiment 13	2.00D	15 cm	200 m	0.25 m	3
Experiment 14	2.00D	25 cm	150 m	0 m	4
Experiment 15	2.00D	35 cm	100 m	0.75 m	1
Experiment 16	2.00D	45 cm	50 m	0.50 m	2

3. Jet Fan Thrust

3.1. Calculation Method for Jet Fan Thrust Reduction Coefficient

The ventilation performance of jet fans critically depends on the boost effect they generate. This effect essentially reflects the complex energy transfer and conversion processes between the fan jet and the existing airflow within the tunnel. This process is influenced by the interaction of momentum between the jet and the tunnel airflow, as well as external factors such as frictional resistance and pressure gradients. Pressure monitoring surfaces 1 and 2 are set at positions 40 m from the tunnel inlet and outlet, respectively. When the jet fan is turned off, the pressures at Sections 1 and 2 can be calculated in FLUENT as P_1 and P_2, respectively. The pressure difference between the two sections (i.e., the flow resistance) is $\Delta P = P_1 - P_2$, which represents the absolute value of the flow resistance difference from Section 1 to Section 2.

When the fan is turned on, the simulated pressures at Sections 1 and 2 rise to P_{1j} and P_{2j}, respectively, with a new pressure difference $\Delta P_j = P_{2j} - P_{1j}$. According to the energy conservation equation, the actual boost pressure of the fan P_{aj} is calculated using the following formula:

$$\Delta P_{aj} = \Delta P + \Delta P_j \tag{1}$$

In calculating the boost pressure of the jet fan, this study extracts the static pressure extremes from the tunnel cross-section before and after the airflow passes through the jet fan, including the minimum and maximum static pressures, and calculates the difference between these two values as the pressure difference (Zhao and Yan, 2016) [19].

The theoretical boost pressure of the jet fan is given by:

$$P_j = n\rho v_j^2 \frac{A_j}{A_r}(1 - \frac{v_r}{v_j}) \tag{2}$$

where n is the number of fans, ρ is the air density, A_j and A_r are the cross-sectional areas of the jet fan (with a fan diameter of 1.12 m) and the tunnel (64.49 m^2), respectively, and V_r and V_j are the ventilation velocities in the tunnel and at the jet fan outlet, respectively.

The boost pressure reduction coefficient η of the jet fan is a key parameter measuring the resistance loss during the development of the air jet. It is defined as follows:

$$\eta = \frac{\Delta P_{aj}}{P_j} \tag{3}$$

3.2. Results of the Calculation of Fan Boost Pressure Reduction Coefficient

Based on the CFD numerical simulations, the boost pressure reduction coefficients for the tunnel models with spiral radii of 500 m, 600 m, 700 m, and 800 m were obtained across 16 × 4 groups of models. The results are shown in Table 4.

Table 4. Boost discount factors for each simulation.

Operating Condition	Experimental Results			
	R = 500 m	R = 600 m	R = 700 m	R = 800 m
1	0.852464	0.836851	0.873807	0.808652
2	0.914686	0.918618	0.906700	0.896843
3	0.866198	0.870198	0.914032	0.872781
4	0.860613	0.861844	0.900049	0.860409
5	0.925400	0.917664	0.945472	0.904130
6	0.837278	0.827340	0.844365	0.789335
7	0.856005	0.868359	0.903476	0.877253
8	0.870874	0.870675	0.883228	0.864291
9	0.894164	0.897620	0.924202	0.885402
10	0.871146	0.882229	0.912920	0.882701
11	0.821841	0.798283	0.842821	0.779051
12	0.883881	0.886202	0.893375	0.878796
13	0.881271	0.901048	0.920138	0.886810
14	0.868672	0.876145	0.935847	0.878456
15	0.898001	0.895940	0.905883	0.888648
16	0.818595	0.798510	0.827719	0.763184

4. Analysis of the Calculation Results of Wind Turbine Boosting Reduction Coefficient

4.1. Range Analysis

Range analysis, as a common analytical method in orthogonal experimental design, is mainly used to evaluate the importance and influence of different factors by comparing the differences in their comprehensive mean values (Liu et al., 2015) [20]. This method believes that the range directly reflects the importance of each factor to the experimental results: a large range indicates a stronger influence, while a small range implies a lower degree of influence. The specific calculation steps are as follows:

(1) Calculate the sum K_i for level i, which represents the sum of boost pressure reduction coefficients for all four trials at level i.
(2) Calculate the average value $\overline{K_i}$ for each factor at the same level.
(3) Calculate the range R for each factor column.

$$R = \max\overline{K_i} - \min\overline{K_i} \tag{4}$$

Based on the experimental results in Table 4, in order to thoroughly explore the importance of each influencing factor and its dynamic trend with the change in spiral tunnel curvature, it is necessary to interpret the orthogonal experimental results using appropriate statistical methods to optimize the layout of jet fan in spiral tunnels. Table 5 shows the range analysis of different operating conditions under the different curvature radii of the tunnels.

Table 5. Range analysis of factors for tunnels with different curvature radii.

Curvature Radius (m)	Factors	Calculation Results			
		L	H	S	K
500	Range	0.006855	0.029834	0.072947	0.007258
	Optimal Level	1.25D	15 cm	100 m	0.75 m
600	Range	0.005794	0.033988	0.089360	0.005266
	Optimal Level	1.25D	15 cm	100 m	0.25 m
700	Range	0.005318	0.039812	0.067149	0.013405
	Optimal Level	1.25D	15 cm	150 m	0 m
800	Range	0.005397	0.029578	0.107049	0.005091
	Optimal Level	1.25D	15 cm	100 m	0 m

When using the boost pressure reduction coefficient of the fan as the evaluation criterion, the following conclusions can be drawn from Table 5:

1. For spiral tunnels with a fixed cross-sectional form, the optimal installation parameters of jet fans are determined. The optimal spacing for the fan group is 1.25D, and the optimal vertical height is 15 cm from the building clearance. However, with changes in the spiral curvature, the optimal offset and longitudinal spacing of the fan group will adjust accordingly.
2. The range analysis results show that the importance order of the factors is: S > H > K, L.
3. For tunnel curvatures of R = 500 m and 600 m, the optimal longitudinal spacing of the fan group is 100 m. When the installation position of the fan group is offset 0.25–0.75 m towards the inner side of the tunnel spiral, the boost effect of the fan group can be enhanced. As the curvature of the spiral tunnel increases, i.e., when R = 700 m, the optimal longitudinal spacing increases to 150 m; however, when R = 800 m, the optimal longitudinal spacing decreases back to 100 m.

4.2. Variance Analysis

Range analysis can identify factors significantly affecting the fan boost pressure, but it cannot distinguish whether data fluctuations are caused by changes in conditions or errors. In contrast, variance analysis offers higher analytical precision, helping to more accurately identify and screen out key factors that truly impact the results (Liu et al., 2015; Wang et al., 2021) [20,21]. The specific steps for variance analysis are as follows:

(1) Calculate the sum of squares for each factor: S_b.

$$S_b = \frac{r}{1}\sum_{i=1}^{m}\left(K_{ij}^2 - \frac{T^2}{n}\right) \tag{5}$$

where (r) is the number of trials at the same level, (K_{ij}) is the sum of the test indices at the same level, (T) is the sum of all test indices, and (n) is the total number of trials.

(2) Calculate the degrees of freedom for each factor:

$$d_b = the\ number\ of\ levels\ for\ each\ factor - 1 \tag{6}$$

(3) Calculate the mean square (M_b) for each factor (if the mean square of the error column is greater than that of the factor columns, the errors need to be combined):

$$M_b = \frac{S_b}{d_b} \tag{7}$$

(4) Calculate the sum of squares of errors (S_e), degrees of freedom (d_e), and mean square (M_b), using the same method to compute the values from the blank column.

(5) Calculate the F value for each factor. The F value is an indicator of the importance of the factor. A larger F value indicates that the factor has a more significant impact on the experimental results.

$$F = \frac{M_b}{M_e} \tag{8}$$

Through the aforementioned calculation process, the F values for each influencing factor in tunnels with different curvature radii can be obtained. The detailed results are listed in Table 6.

Table 6. Analysis of variance.

Radius of Curvature/m	Parameters	Calculation Results			
		L	H	S	K
500	F value	1.772600	29.366829	139.588004	1.741588
600		-	26.214170	150.643000	-
700		-	8.943584	34.314700	-
800		-	25.675150	0.000096	-

In Table 6, the *F* value reflects the level of importance of the factors, with larger *F* values indicating a greater impact of the factors on the experimental results. From Table 6, it can be observed that the longitudinal spacing and vertical height of the fans have a significant impact on the boosting ability, while within the specified range of this experiment, the lateral offset and spacing have a minor impact on the boosting ability. Additionally, the order of importance of each factor is consistent with the conclusions drawn from the range analysis in Section 4.1.

5. Optimal Recommendations for Spatial Layout of Jet Fan Groups in Spiral Tunnel

5.1. Spiral Tunnel Longitudinal Jet Flow Distribution Patterns

The optimal installation parameters for the fans inside the spiral tunnel, evaluated based on the boosting capacity, are detailed in Table 7.

Table 7. Values of factors influencing the optimal boost factor for tunnels with different curvatures.

Curvature Radius (m)	Factors				
	L	H	S	K	Order of Influence
$R = 500$	1.25D	15 cm	100 m	0.75 m	S > H > K > L
$R = 600$	1.25D	15 cm	100 m	0.25 m	S > H > K > L
$R = 700$	1.25D	15 cm	150 m	0 m	S > H > K > L
$R = 800$	1.25D	15 cm	100 m	0 m	S > H > L > K

Jet ventilation design needs to consider factors such as cable losses and fan maintenance. Typically, fans are arranged in a concentrated manner, ensuring sufficient distance between fan groups to avoid performance interference. Therefore, in this section, a spiral tunnel with a length of 700 m was selected to study the effect of the longitudinal spacing of jet fans on ventilation performance. Since, in this scenario, the longitudinal spacing of fans has a significant impact compared to lateral offset and spacing on the boosting capability, factor H = 15 cm was fixed according to Table 3, and four sets of experiments (Experiment 1, 5, 9, 13) were selected for observation, temporarily disregarding the influence of lateral offset and spacing on ventilation performance.

Based on the observation from Figure 6, when the longitudinal spacing between the two groups of fans is set to 50 m and 100 m, the velocity in front of the second group of fans exceeds 7.5 m/s, which has not yet fully decreased to the average wind speed of the tunnel section. A smaller longitudinal spacing may lead to mutual interference between adjacent jets, resulting in a cross-effect and the formation of a complex flow field structure, thereby affecting the ventilation effect. However, when the longitudinal spacing increases to 150 m and 200 m, the velocity in front of the second group of fans has basically decreased to the level of the average velocity of the tunnel section. A larger longitudinal spacing may make the jets relatively independent, and the flow field tends to be more stable. However, excessively large spacing may increase system investment and operating costs, thereby affecting the economy of the ventilation system. Within the longitudinal spacing of the two groups of fans, the fluid shows a trend of increasing velocity at different positions and then decreasing (Zhao and Yan, 2016) [19]. This is because the arrangement of jet fans and the spiral line shape in the spiral tunnel jointly affect the airflow characteristics. The fluid in the tunnel will go through the stages of jet development and reverse pressure flow.

Figure 7 illustrates the variation in the trend of the longitudinal average cross-sectional static pressure at different cross-sectional positions when the fan group is distributed at different curvature radii. Since the influence of the longitudinal spacing of the fans on the boosting capability is significant compared to the lateral offset and spacing relative to the vertical height, when studying the effect of curvature radius on the longitudinal spacing of the fan group, the vertical height should be fixed, and the influence of the lateral offset and spacing on the boosting capability should be temporarily disregarded. Therefore, when R = 500 m, 600 m, and 800 m, Experiment 5 from orthogonal Table 3 is selected (S = 100 m, H = 15 cm, L = 1.50D, K = 0.50 m); when R = 700 m, Experiment 9 from orthogonal Table 3 is selected (S = 150 m, H = 15 cm, L = 1.75D, K = 0.75 m). From the figure, it can be observed that the initial static pressure level is relatively low before reaching a distance of 50 m from the entrance of the tunnel. As the airflow approaches the jet fan and is subjected to its suction effect, the static pressure shows a significant decrease. However, after passing through the fan, due to the exchange of momentum between the jet and the tunnel airflow, the static pressure gradually recovers and increases. Near the position of the second fan group, the static pressure reaches its peak, indicating the effective utilization of the jet effect. Similar phenomena are observed before and after the airflow reaches the second fan group. Due to the coupling effect of multiple factors, the length of the jet in different curvature tunnels varies as the airflow passes through the first fan group and is pressurized. When R = 500 m, the spiral tunnel reaches its maximum static pressure of −21.89 Pa at a distance of 90 m from the entrance of the first fan group; when R = 600 m, it reaches its maximum static pressure of −21.58 Pa at a distance of 85 m from the entrance of the first fan group; when R = 700 m, it reaches its maximum static pressure of −18.50 Pa at a distance of 130 m from the entrance of the first fan group; when R = 800 m, it reaches its maximum static pressure of −20.72 Pa at a distance of 85 m from the entrance of the fan group. According to Table 5, adjusting the lateral spacing of the fan to 1.25D at this time and offsetting the fan group towards the inside of the tunnel by 0.25~0.75 m when R < 700 m can enhance the boosting effect of the jet fan. Therefore, in the layout of spiral tunnels, optimizing the configuration of fans can adjust their longitudinal range of action, thereby mitigating the negative effects that may arise from the curvature of the tunnel.

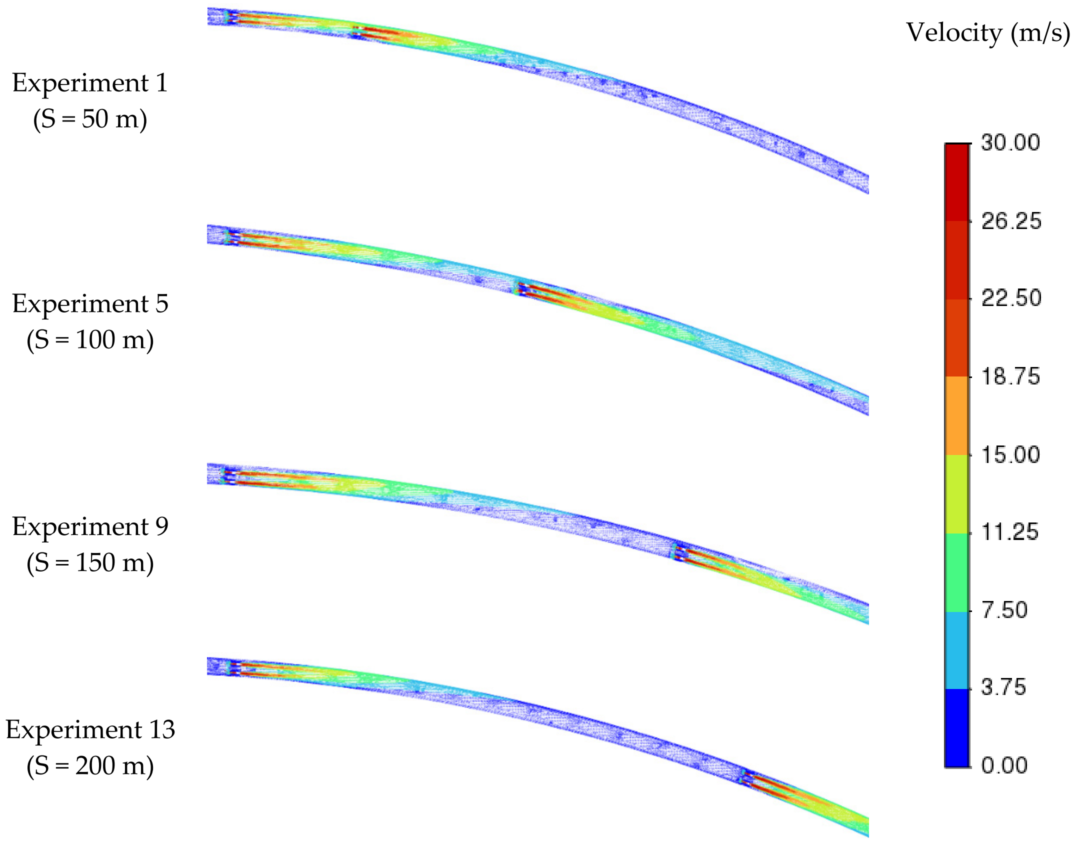

Figure 6. Vector diagram of wind speed in different experimental spiral tunnels (R = 700 m).

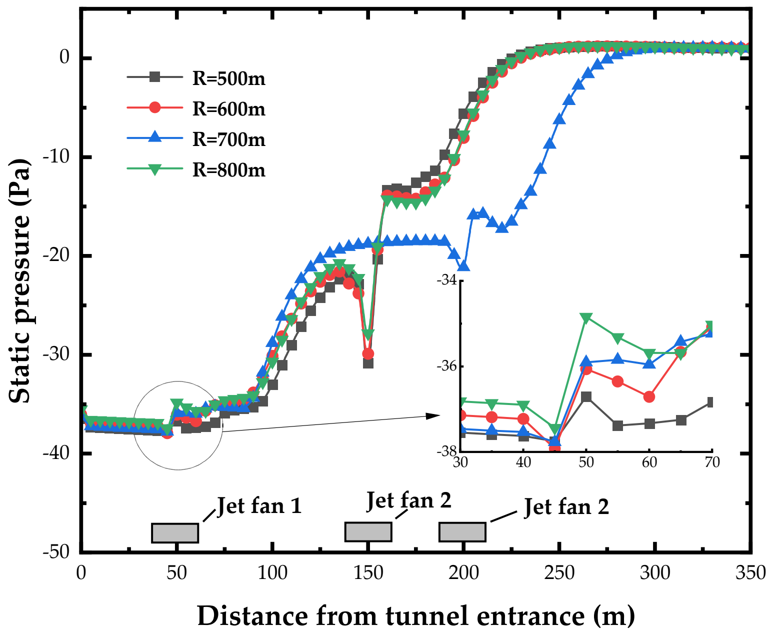

Figure 7. The average static pressure along the cross-section of a tunnel under different curvature radii.

When designing orthogonal experiments, the wide intervals of longitudinal spacing values may lead to large variances in the results. Through range analysis, a broad range of longitudinal spacing values is obtained. Therefore, we consider optimizing the experimental design by narrowing the range of longitudinal spacing values to improve the repeatability and accuracy of the results. Thus, each spiral tunnel with different curvatures is designed based on the optimal values of each factor in Table 7. Figure 8 shows the variation in the trend of longitudinal average cross-sectional static pressure when the fan groups are distributed at different section positions under different curvature radii. From Figure 8, it can be observed that when R = 500 m, the spiral tunnel reaches its maximum static pressure of −22.03 Pa at a distance of 90 m from the entrance of the first fan group; when R = 600 m, it reaches its maximum static pressure of −23.59 Pa at a distance of 90 m from the entrance of the first fan group; when R = 700 m, it reaches its maximum static pressure of −18.37 Pa at a distance of 135 m from the entrance of the first fan group; when R = 800 m, it reaches its maximum static pressure of −21.34 Pa at a distance of 90 m from the entrance of the fan group. By comparing and analyzing Figures 7 and 8, it is found that optimizing the lateral offset and spacing does not significantly affect the longitudinal spacing of the fan groups, with an increase of at most 5 m, indirectly indicating the accuracy of the orthogonal experiments.

When using boosting capacity as the evaluation criterion, the relationship between the spiral radius and the longitudinal spacing of fan groups is depicted in Figure 9.

The fitting equation for the relationship between fan longitudinal spacing and spiral radius, obtained using the polynomial fitting function of Origin2021 software, is represented as follows:

$$f(x) = 5435.1 - 26.2845x + 0.04232x^2 - 2.2275 \times 10^{-5}x^3 \tag{9}$$

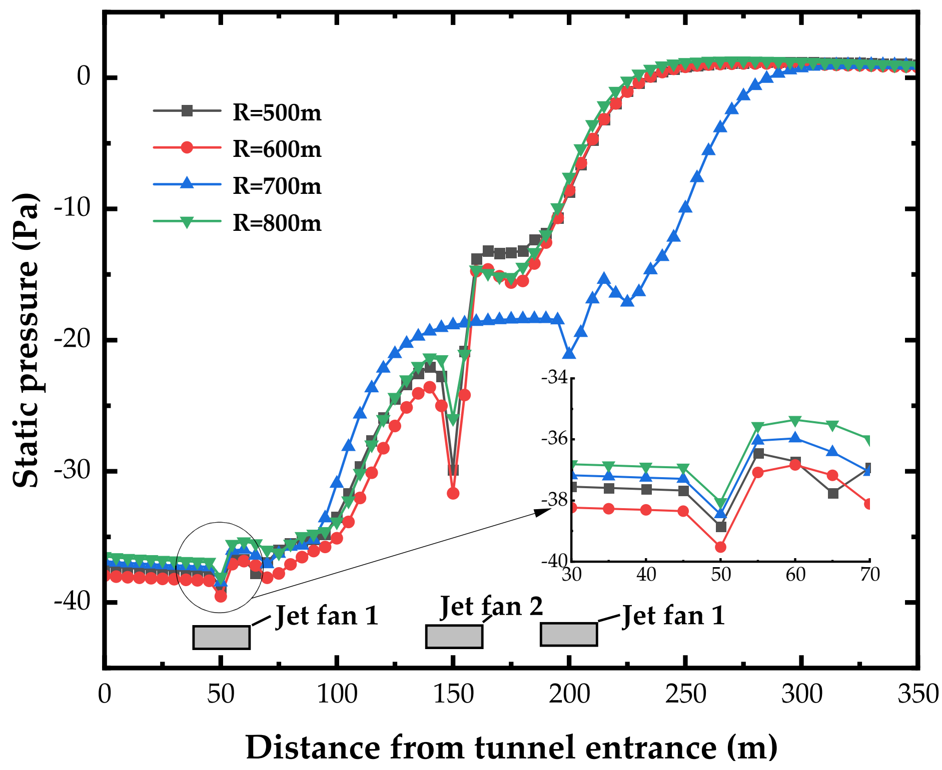

Figure 8. Average static pressure along the tunnel section for different radii of curvature (optimal level).

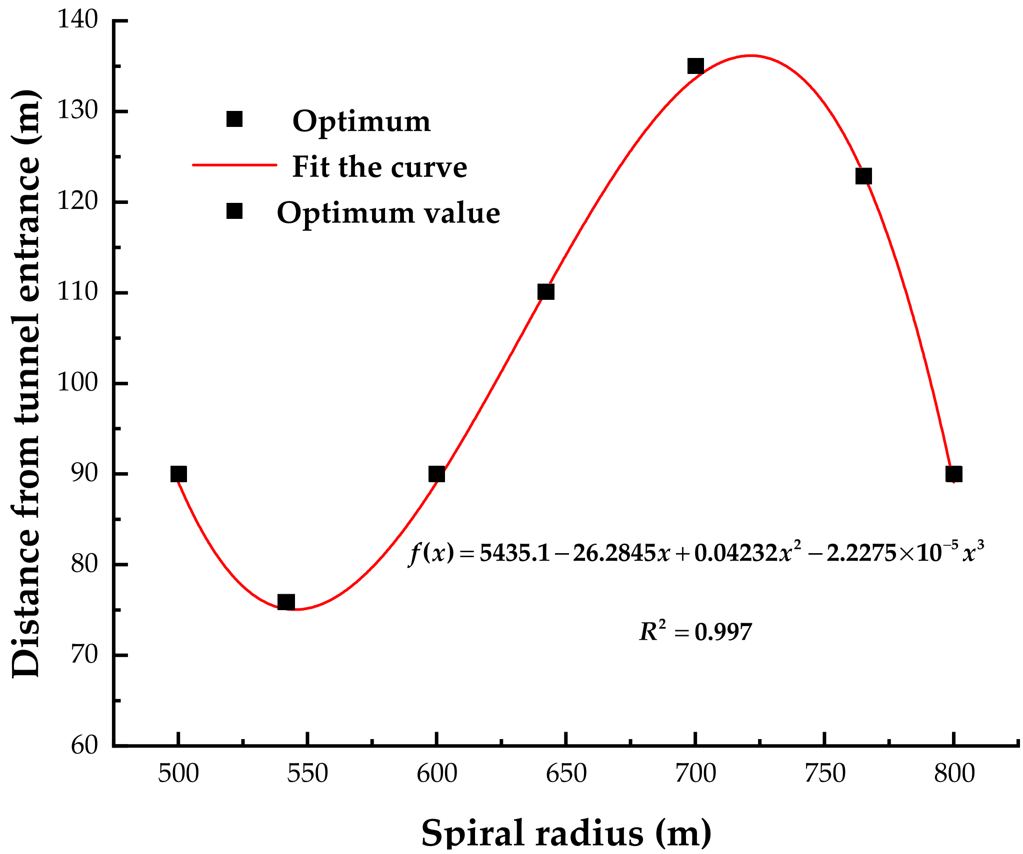

Figure 9. Longitudinal spacing curve for spiral tunnel wind turbines.

5.2. Spiral Tunnel Cross-Sectional Jet Distribution Law

From Table 7, it can be observed that when R = 500 m, R = 600 m, and R = 700 m, the degree of influence of each factor on the fan pressure is in the order of S > H > K > L. In order to explore the influence of the vertical height of the fan on the flow field distribution in the cross-sectional position of the fan group, this chapter adopts the method of controlling variables. A model with a spiral radius of S = 150 m, L = 1.75D, and K = 0.75 m is selected, and only the vertical height of the fan is changed, set to H = 15 cm, 25 cm, 35 cm, and 45 cm, respectively.

From Figures 10 and 11, it can be observed that in the initial stage of the jet (at 10 m), the velocity profile reveals two significant free jet characteristics. The jet core region exhibits higher velocity values, while the annular region at the cross-section periphery records relatively lower velocity levels. When the fan is positioned 15 cm from the construction clearance, the velocity stratification in the jet core region is above 3.75 m/s, and the arch top is in contact with the jet area. As the vertical height of the fan increases, the fan's position gets closer to the arch top, resulting in noticeable contact between the arch top and the 3.75~7.50 m/s velocity stratification when the fan is positioned 45 cm from the construction clearance.

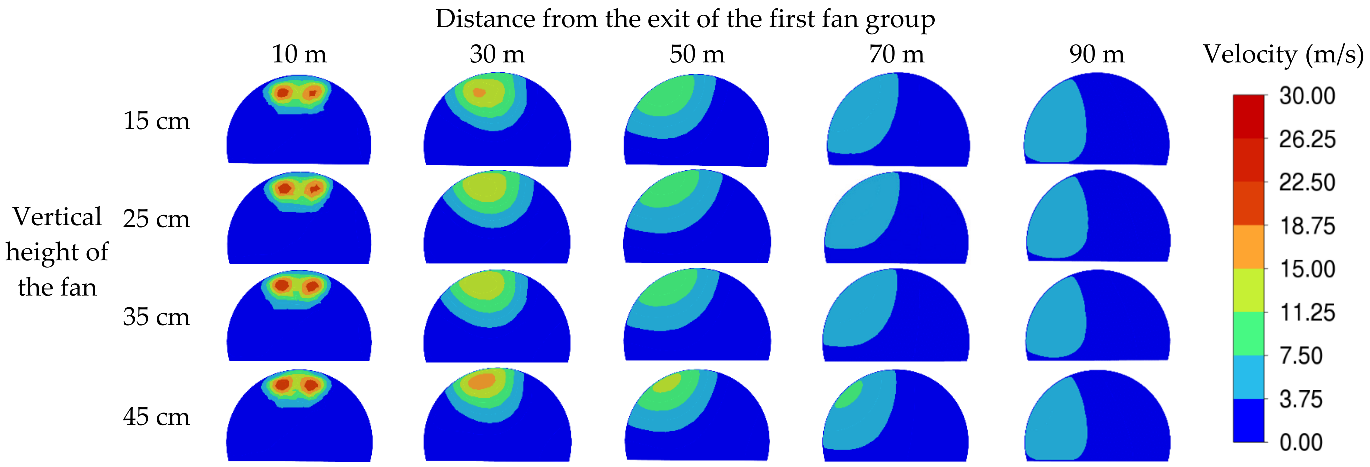

Figure 10. Development of tunnel jets at different vertical heights of the wind turbine.

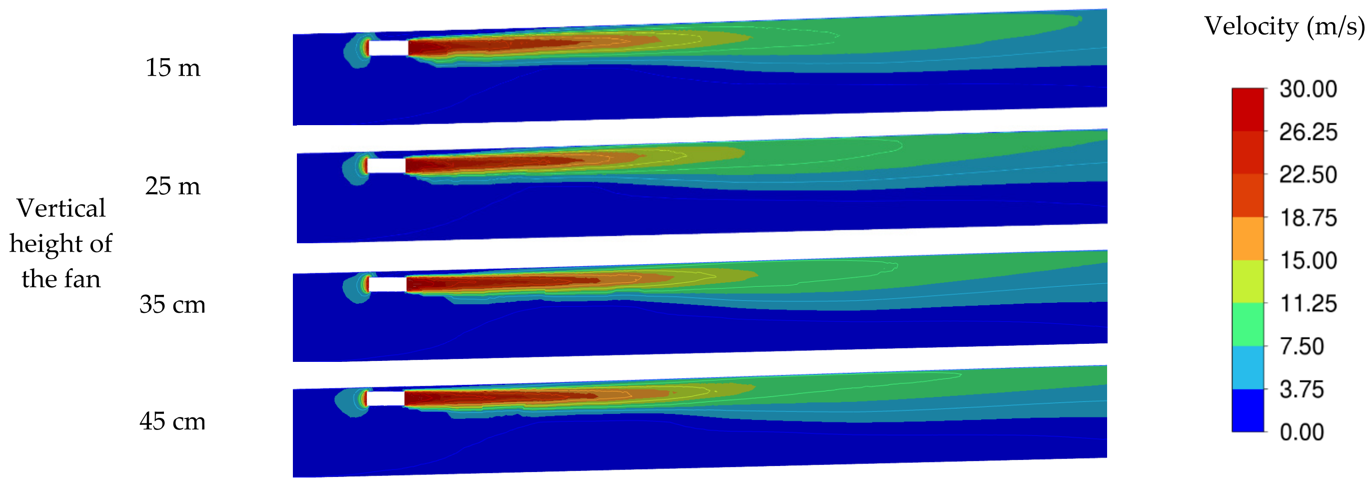

Figure 11. Velocity changes along the turbine axial profile at different vertical heights.

When the fan is positioned at heights of 25 cm and 35 cm from the construction clearance, the airflow speed at 30 cm from the fan outlet is significantly lower than that at 15 cm from the construction clearance. This phenomenon is due to the restriction imposed by the tunnel arch top on the airflow from the fan outlet, limiting its upward expansion capability. When the airflow collides with the tunnel arch top or experiences friction from the tunnel walls, the high-speed airflow loses considerable kinetic energy. This energy loss leads to a decrease in performance for the low-speed airflow that is not effectively captured by the fan (Axel et al., 1997) [22].

From a fluid dynamics perspective, the higher the installation position of the fan, the weaker the resulting pressurization effect. However, when the fan is positioned 45 cm from the construction clearance, the wind speed in the range of 30 cm to 70 cm from the fan outlet is slightly higher than when the fan is positioned 15 cm from the construction clearance. This is because the fan is too close to the arch top, causing the emitted airflow to collide with the arch top prematurely. Although this results in some energy and kinetic energy loss, the Coanda effect causes the airflow to have a smaller diffusion area in the longitudinal space within a certain distance. According to the continuity equation in fluid mechanics (the average velocity of the flow beam cross-section is inversely proportional to the cross-sectional area of the flow), the average velocity of this cross-section will instead increase.

Even though the fan is farther from the arch top and the airflow might be somewhat restricted, it can maintain its kinetic energy and effectively propel through the entire jet path. Therefore, the configuration of the fan being positioned 15 cm from the construction clearance seems more suitable for maintaining good ventilation within the tunnel. This configuration helps to alleviate the burden on the tunnel ventilation system.

To investigate the relationship between the jet development in the tunnel and the change in the lateral spacing of the fans, the velocity contour maps under different lateral spacings along the fan axis are shown in Figure 12.

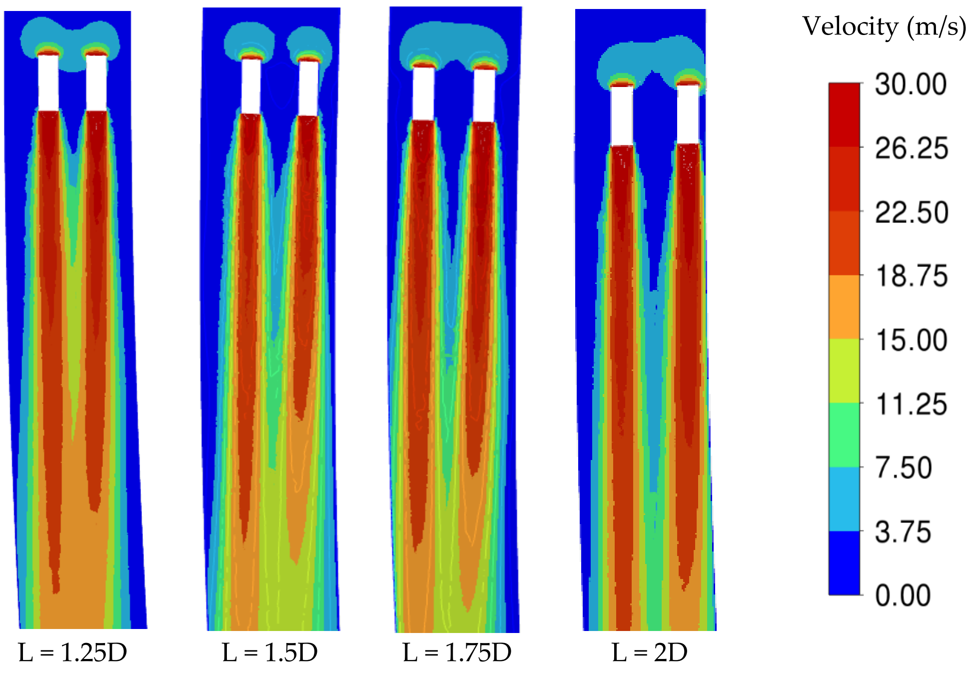

Figure 12. Variation in wind turbine speed at different transverse spacing along the wind turbine axis cloud plot (R = 700 m).

From Figure 12, it can be seen that when the fan spacing and lateral offset are too large, the fans, being close to the tunnel walls, cause excessive kinetic energy loss due to friction. This is because excessive fan lateral spacing and offset lead to uneven airflow distribution, creating local blockages and vortices that alter the airflow direction, reducing ventilation efficiency, and increasing the energy consumption of the ventilation system. Therefore, reasonable adjustments of lateral offset and fan group spacing will help optimize the ventilation system design, reduce local velocity gradients, and lower energy consumption. Adjusting the fan group spacing can influence the interaction between the high-speed jets emitted by the fans, thereby affecting the pressurization effect. Shifting the fan groups to find the optimal cross-sectional lateral arrangement can reduce the impact of the tunnel profile on jet development (Li, 2004) [23]. Therefore, in design and operation, it is necessary to accurately control the position of the fan groups, using advanced techniques such as wind tunnel tests and numerical simulations to ensure a reasonable arrangement of fan groups, providing uniform and effective ventilation suitable for the complex aerodynamic environment of spiral tunnels.

From Figure 13, it can be observed that the optimal lateral offset values of the fan groups under different curvature radii (R = 500 m, 600 m, 700 m, 800 m) correspond to the optimal levels of 4, 2, 1, and 1, respectively, with offset values of 0.75 m, 0.25 m, and 0 m. This shows that the larger the tunnel curvature radius, the smaller the optimal lateral offset of the fan group. This is because a larger curvature radius indicates a less pronounced curve, causing the airflow to tend more towards linear flow. In this situation, the jet generated by the fan is relatively concentrated and has a weaker impact on the flow, resulting in a smaller optimal lateral offset. Conversely, when the curvature radius is smaller, the curve is steeper, requiring greater centripetal force for the airflow to follow the curve. In this case, the jet produced by the fan is more strongly influenced by the centripetal force, leading to the faster outward diffusion of the jet and larger local velocity gradients, thus necessitating a larger lateral offset.

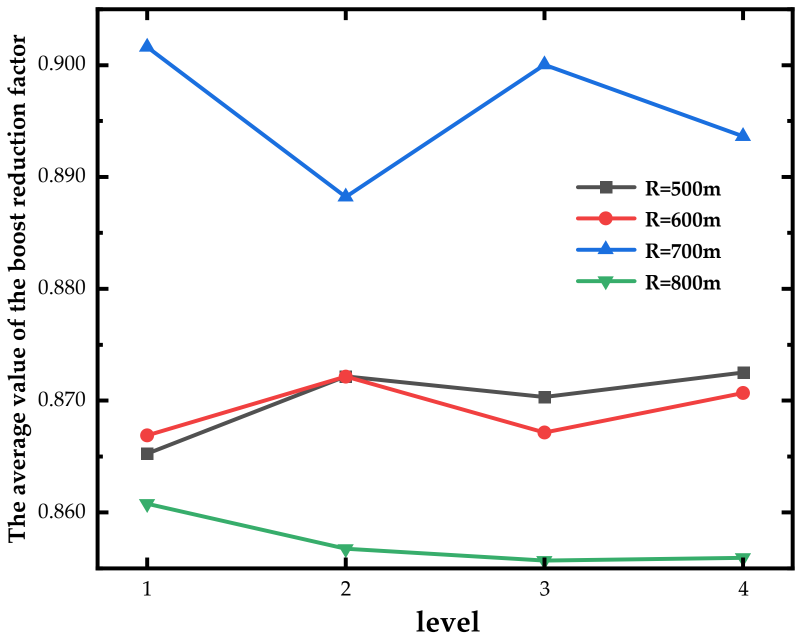

Figure 13. Plot of factor levels versus average boost discount factor.

Therefore, as the curvature radius increases, the optimal lateral offset of the fan groups in the ventilation system decreases. This helps to maintain a more uniform ventilation effect and improves the efficiency and performance of the ventilation system.

When using boosting capability as the evaluation criterion, the relationship between the spiral radius and the lateral offset of the fan groups can be seen in Figure 14.

The fitting equation between the lateral offset of the fans and the spiral radius using the polynomial fitting function in Origin software is expressed as follows:

$$f(x) = \frac{0.75}{1 + 10^{-0.01667 \times (575 - x)}} \tag{10}$$

The recommended installation parameters of the fans in the spiral tunnel, evaluated based on the boosting efficiency, are detailed in Table 8.

Table 8. Evaluation of the optimum value of boosting capacity.

Curve Radius (m)	Factors			
	L	H	S	K
$R = 500$	1.25D	15 cm	90 m	0.75 m
$R = 600$	1.25D	15 cm	90 m	0.25 m
$R = 700$	1.25D	15 cm	135 m	0 m
$R = 800$	1.25D	15 cm	90 m	0 m

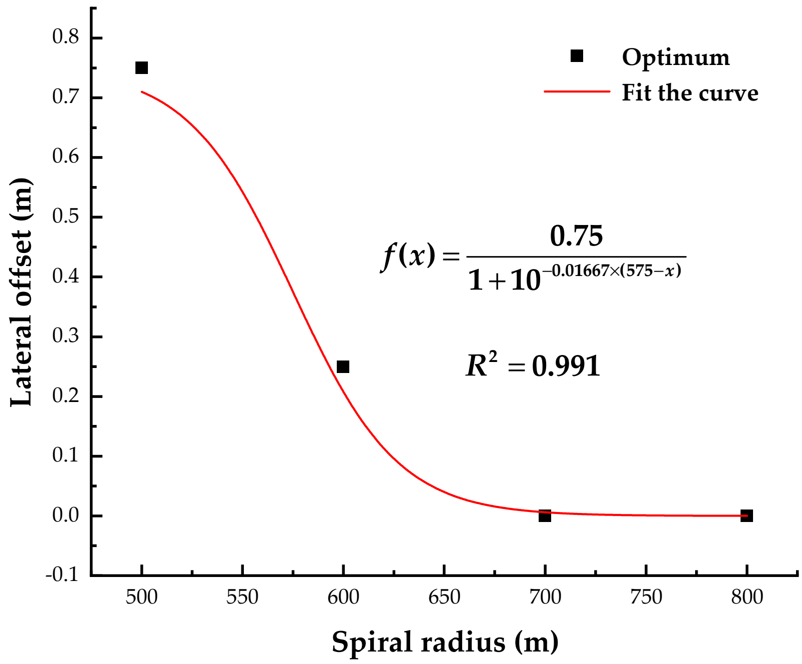

Figure 14. Spiral tunnel wind turbine lateral offset curve.

6. Conclusions

Combined with orthogonal experiments, this study investigated the influence of different helical curvature radii on the optimal spatial layout parameters of jet fan units under the coupling effect of multiple factors. The research findings indicate:

(1) In high-altitude helical tunnels, the optimization of jet fan spatial layout is closely related to the tunnel's helical curvature. For high-altitude tunnels with R = 500 m, 600 m, 700 m, and 800 m, this study successfully determined the optimal layout scheme of jet fans, as well as establishing the relationship expression between helical radius and the lateral offset and longitudinal spacing of fan units, providing important reference for the design of future similar projects.

(2) When R = 500 m, 600 m, 700 m, the degree of influence of each factor on the fan's boost pressure is S > H > K > L, with L having the least impact on the boost reduction coefficient. However, when R = 800 m, the degree of influence of each factor on the fan's boost pressure is S > H > L > K, with K having the least impact on the boost reduction coefficient.

(3) Under different tunnel curvature conditions, the optimal values for fan group spacing and vertical height are fixed; the optimal fan group spacing is 1.25D, and the optimal vertical height is 15 cm from the building limit boundary. For different curvature radii, the optimal longitudinal spacing of fan groups is 90 m, 90 m, 135 m, and 90 m, respectively. By offsetting the installation of fan groups towards the inside of the tunnel spiral by 0 to 0.75 m (R < 700 m), the boost efficiency of fan groups can be enhanced.

Author Contributions: Conceptualization, Z.W. and H.L.; Data curation, B.Z. and C.J.; Funding acquisition, Z.W.; Investigation, Q.L. and L.W.; Methodology, H.L., B.Z. and S.W.; Project administration, Z.W., L.W. and C.J.; Resources, C.J.; Software, Q.L. and L.W.; Supervision, B.Z. and S.W.; Validation, Q.L., H.L., S.W. and C.J.; Visualization, S.W.; Writing—original draft, Z.W. and L.W.; Writing—review and editing, Q.L., H.L. and B.Z. All authors have read and agreed to the published version of the manuscript.

Funding: This research was funded by the Science and Technology Research Program of Chongqing Municipal Education Commission (Grant Nos. KJZD202204001).

Data Availability Statement: Data is contained within the article.

Conflicts of Interest: Author Chaolin Jia was employed by the company Chongqing Chuanjiu Construction Co., Ltd. The remaining authors declare that the research was conducted in the absence of any commercial or financial relationships that could be construed as a potential conflict of interest.

References

1. Xu, Z.; Wang, B.; Kong, J.; Chen, T.; Liang, Y. Study on the Influence of Transverse Layout Spacing of Fans on the Distribution of Pollutants in Highway Tunnels. *J. Saf. Environ.* **2021**, *21*, 321–327.
2. Davies, P.O.; Fisher, M.J.; Barratt, M.J. The characteristics of the turbulence in the mixing region of around jet. *J. Fluid Mech.* **1963**, *15*, 337–367. [CrossRef]
3. Mutama, K.A.; Hall, A.E. The experimental investigation of the fan aerodynamics using wind tunnel modeling. *J. Fluids Eng.* **1996**, *118*, 322–328. [CrossRef]
4. Wang, F.; Wang, M.; He, S.; Zhang, J.; Deng, Y. Computational study of effects of jet fans on the ventilation of a highway curved tunnel. *Tunn. Undergr. Space Technol.* **2010**, *25*, 382–390. [CrossRef]
5. Wang, F.; Wang, M.N.; Wang, Q.Y. Numerical study of effects of deflected angles of jet fans on the normal ventilation in a curved tunnel. *Tunn. Undergr. Space Technol.* **2012**, *31*, 80–85. [CrossRef]
6. Li, Y.; Chen, T.; Xu, Z.; Kong, J.; Wang, M.; Fan, C. Influence of winding wall on the entrainment characteristics of air jet in curved road tunnels. *Tunn. Undergr. Space Technol.* **2019**, *90*, 330–339. [CrossRef]
7. Ding, M.; Wang, B.; Zeng, Y. Numerical Simulation Study on the Boosting Characteristics of Jet Fans in Large Underground Interchange Tunnels. *Highways* **2017**, *62*, 248–254.
8. Chen, Y.; Wang, T.; Tao, H.; Xu, Z. Research on Ventilation Efficiency Optimization of Jet Fans in Curved Tunnels. *Fire Sci. Technol.* **2021**, *40*, 977–982.
9. Xu, Z.; Tao, H.; Wang, T.; Hou, L. Study on the Influence of Tunnel Curvature Radius on Air Jet Flow Field Characteristics and Boosting Efficiency. *J. Saf. Environ.* **2023**, *23*, 415–423.
10. Chen, T.; Zhou, D.; Lu, Z.; Li, Y.; Fan, C. Study of the applicability and optimal arrangement of alternative jet fans in curved road tunnel complexes. *Tunn. Undergr. Space Technol.* **2021**, *108*, 103721. [CrossRef]
11. Chen, K.; Ren, J.; Ma, F.; Guo, H.; Kang, J.; Yang, S.; Zhuang, T.; Lei, Y. Study on the Influence of Tunnel Curvature on Installation Parameters of Jet Fans in High-altitude Tunnels. *J. Undergr. Space Eng.* **2021**, *17*, 608–617.
12. Li, Q.; Wan, Y.; Wang, X.; Li, M.; Wang, F.; Yang, C. Study on Optimization of Fan Layout in Small-radius Curved Tunnel Considering Multi-factor Coupling Effects. *J. Saf. Environ.* **2023**, *23*, 4308–4317.
13. Rosso, M.M.; Cucuzza, R.; Marano, G.C.; Aloisio, A.; Cirrincione, G. Review on deep learning in structural health monitoring. In *Bridge Safety, Maintenance, Management, Life-Cycle, Resilience and Sustainability*; CRC Press: Boca Raton, FL, USA, 2022; pp. 309–315.
14. Habashneh, M.; Cucuzza, R.; Domaneschi, M.; Rad, M.M. Advanced elastoplastic topology optimization of steel beams under elevated temperatures. *Adv. Eng. Softw.* **2024**, *190*, 103596. [CrossRef]
15. Rosso, M.M.; Aloisio, A.; Cucuzza, R.; Pasca, D.P.; Cirrincione, G.; Marano, G.C. Structural health monitoring with artificial neural network and subspace-based damage indicators. In *International Conference on Trends on Construction in the Post-Digital Era*; Springer International Publishing: Cham, Switzerland, 2022; pp. 524–537.
16. Wang, F. Research on Key Parameters of Operation Ventilation in Curved Highway Tunnels. Doctoral Dissertation, Southwest Jiaotong University, Chengdu, China, 2010.
17. Wang, Y. Numerical Simulation Research on Longitudinal Ventilation of Changda Highway Tunnel. Master"s Thesis, Chang'an University, Xi'an, China, 2000.
18. *JTG/TD70/2-02-2014*; Guidelines for Highway Tunnel Ventilation Design. Ministry of Transport of the People's Republic of China: Beijing, China, 2014.
19. Zhao, L.; Yan, Z. CFD Analysis of Spatial Layout Optimization of Jet Fans in Two-Lane Highway Tunnel. *Tunn. Constr.* **2016**, *36*, 411–417.
20. Liu, D.; Tang, Y.; Li, B.; Peng, W. Numerical Simulation and Experimental Study on Optimization of Ventilation Duct for Gas Tunnel Construction. *China J. Highw. Transp.* **2015**, *28*, 98–103+142.
21. Wang, L.; Zhong, Y.; Li, L.; Li, M. Optimization of Press-in Ventilation for Gas Tunnel Based on Orthogonal Experiment. *Mod. Tunneling Technol.* **2021**, *58*, 170–178.

22. Bring, A.; Malmström, T.G.; Boman, C.A. Simulation and measurement of road tunnel ventilation. *Tunn. Undergr. Space Technol.* **1997**, *12*, 417–424. [CrossRef]
23. Li, J. A Summary of Design and Type Selection of Jet Fan in Highway Tunnels. *Highway* **2004**, 0451-0712(2004)03-0141-04.